Study on Optimal Calibration Configurations of a Parallel Type Machining Center Under a Single Planar Constraint

Min Ki Lee*, Tae Sung Kim, Kun Woo Park

Department of Control and Instrumentation Engineering Changwon National University, Kyungnam 641-773, Korea

This paper examines the parameter observability of a calibration system that consrains a mobile platform to a planar table to take the calibration data. To improve the parameter observability, we find the optimal configurations providing the calibration with maximum contribution. The QR-decomposition is used to compute the optimal configurations that maximize the linear independence of rows of an observation matrix. The calibration system is applied to the parallel type manipulator constructed for a machining center. The calibration results show that all the necessary kinematic parameters assigned in a Stewart-Gough platform are identifiable and convergent to desirable accuracy.

Key Words : Kinematic Parameter, Observability, Observation Matrix, Optimal Calibration Configuration

1. Introduction

Kinematic calibration is performed to identify the actual parameters, which are used minimize the errors between actual movements and theoretical movements. The main issue of calibration is the development of a precise measurement system to perceive the actual movements. The actual pose of the platform is measured by external devices such as laser (Zhuang et al., 1992), theodolite (Zhuang et al., 1995; Masory and Jiahua, 1995) and inclinometer (Desnard and Khalil, 1999). These methods can directly measure the pose of a platform, i.e., the calibration target. But it is expensive to obtain the accurate measurements in the 3D space. Here, we can consider an easy way to perceive the errors : 1) constraint movements are defined ; 2) active joint displacements are read when a platform satisfies the constraint movements ; 3) a kinematic model computes a theoretical movement ; 4) the error is found from the difference between the theoretical movement and the pre-defined constraint movement. The measurement system for the constraint movement needs only a simple sensing device to check whether the constrained movement is done completely. In this research the calibration system which constrains the movement of a platform by a single planar table and digital indicators is developed. The calibration system uses only one mechanical fixture so that it can avoid the problem arising from the misalignment of multiple fixtures. But it seems to cause poor parameter observability due to the constrained movements and the local calibration due to a single planar table. The optimal configurations that offer the maximum contribution to calibration are found by the QR-decomposition (Besnard and Khalil, 2001) : the linear independence measure is obtained by summing the reciprocals of diagonal elements of $\mathbf{R}$ matrix and the optimal configurations are found to maximize the independence measure. The calibration system is applied to the parallel type manipulator constructed for a machining center. The calibration results indicate

* Corresponding Author,
E-mail : minkiee@sarim.changwon.ac.kr
TEL : +82-55-275-7553; **FAX** : +82-55-262-5064
Department of Control and Instrumentation Engineering Changwon National University, Kyungnam 641-773, Korea. (Manuscript **Received** December 12, 2002; **Revised** October 8, 2003)

that all the necessary kinematic parameters assigned in the Parallel type Machining Center (PMC) are identifiable. Moreover, changing the height of digital indicators mounted on the mobile platform can shift the levels of constraint plane for the global calibration. This verifies that the calibration system is an effective, low cost and feasible technique for a Parallel typed Machining Center in an industrial environment.

2. Calibration System with Constraint Operators

The platform is placed arbitrarily in an unconstrained coordinate while being fixed in a constrained coordinate. Here, *twist* coordinates are employed to describe the constraint movement (Hunt, 1978). While a body is moving in space, its movement is represented by 6-components of twist coordinates:

$$\mathbf{T}=[T_1,\ T_2,\ T_3,\ T_4,\ T_5,\ T_6]^T \tag{1}$$

where T_1, T_2 and T_3 are the components of the angular velocity of the body, and T_4, T_5 and T_6 are those of the linear velocity. A *constraint operator*, $\boldsymbol{C}[.]$ is introduced to define the constraint movement between the two configurations in bracket, [.]. When a platform moves from configurations $\boldsymbol{\chi}^a$ to $\boldsymbol{\chi}^b$ under $\boldsymbol{C}$, the constraint movement is defined as:

$$\boldsymbol{C}[\boldsymbol{\chi}^b(\triangle\mathbf{q}^b,\ \boldsymbol{\rho})-\boldsymbol{\chi}^a(\triangle\mathbf{q}^a,\ \boldsymbol{\rho})]=\mathbf{N} \tag{2}$$

where the vectors $\triangle\mathbf{q}$ and $\boldsymbol{\rho}$ represent the active joint displacements and the actual kinematic parameters, respectively,

$$\boldsymbol{C}=\mathrm{diag}(c_1,\ c_2,\ \cdots,\ c_6)$$
$$\boldsymbol{N}=[n_1,\ n_2,\ \cdots,\ n_6]^T$$

c_j for $j=1,\ \cdots,\ 6$ is 1 if the j-th coordinate of *twist* is constrained. Otherwise, it is 0, and n_j for $j=1,\ \cdots,\ 6$ is defined by

$$n_j=0 \text{ for } c_j=0 \tag{3a}$$

$$n_j={}^d n_j+\hat{n}_j \text{ for } c_j=1 \tag{3b}$$

where ${}^c n_j$ is the corresponding constraint movement and $\hat{n}_j$ is the error coming from the mechanical fixture such as measurement noise, etc.. From the constraint movements, the calibration equation is derived as follow:

$$\mathrm{G}(\triangle\mathbf{Q},\ \sum,\ \boldsymbol{\rho})=\begin{bmatrix} g_1(\triangle\mathbf{q}^{0\to1},\ \mathbf{N}^1,\ \boldsymbol{\rho}) \\ \vdots \\ g_e(\triangle\mathbf{q}^{e-0\to e},\ \mathbf{N}^e,\ \boldsymbol{\rho}) \end{bmatrix}=0 \tag{4}$$

where $\triangle\mathbf{Q}=[\triangle\mathbf{q}^{0\to1},\ \cdots,\ \triangle\mathbf{q}^{e-1\to e}]^T$ contains $\triangle\mathbf{q}$ for e different configurations, and $\sum=[\mathbf{N}^1,\ \cdots,\ \mathbf{N}^e]^T$ are the constraint movements. The nominal kinematic parameters are denoted by the vector $\boldsymbol{\rho}_0$ while $\triangle\boldsymbol{\rho}$ is the error vector (thus we have $\boldsymbol{\rho}=\boldsymbol{\rho}_0+\triangle\boldsymbol{\rho}$). It can be linearized at $\boldsymbol{\rho}_0$ to yield the error model:

$$\triangle\mathbf{H}(\triangle\mathbf{Q},\ \sum,\ \boldsymbol{\rho}_0)=\mathbf{J}(\triangle\mathbf{Q},\ \sum,\ \boldsymbol{\rho}_0)\triangle\boldsymbol{\rho} \tag{5}$$

where $\triangle\mathbf{H}$ is the error of the kinematic model and $\mathbf{J}$ is the $(r\times p)$ observation matrix, while p is the number of kinematic parameters and $r\gg p$: $r=k*e$ where $k=\sum_{j=1}^{6}c_j$ is the number of constraint coordinates. The observation matrix $\mathbf{J}$ can be calculated numerically by supposing a small variation of ε on each kinematic parameter and computing the corresponding differential changes.

3. Parameter Observability Under Constrained Movement

All the kinematic parameters may not be identified under a constraint movement because some of the parameters have no effect on the movements and some others are grouped together. To improve the parameter observability, we take the optimal configurations to attain maximum contribution to the calibration. An early study of optimal configurations (Borm and Menq, 1991) maximized the observability measure (Menq et al., 1989), which is defined by the relationship between the magnitude of singular values and the number of kinematic parameters. The simulation results showed that the configurations influence the calibration results more than the number of calibration equations does. Currently, Besnard and Khalil (2001) used the QR-decomposition of the observation matrix to examine the identifiable parameters of a Stewart-Gough Parallel

robot.

This research uses the QR-decomposition to find a succeeding optimal configuration where the corresponding rows of the observation matrix maximize the linear independence of the other rows. The configuration is changed from χ^i to χ^{i+1} by a free vector $\mathbf{F}$ defined as the complement of C:

$$\mathbf{F}(\triangle\mathbf{q}^{i\to i+1}, \boldsymbol{\rho}) = \bar{C}[\chi^{i+1} - \chi^i] \tag{6}$$

The vector $\mathbf{F}$ possesses a degrees of freedom as many as the number of the unconstrained coordinates, i.e., $\bar{k} = \sum_{j=1}^{6} \bar{c}_j$ and its component f_j for $\bar{c}_j = 1$ is chosen to yield the calibration equation $g_{i+1}(\mathbf{F})$. From the constraint movement between configurations χ^i and χ^{i+1}, the rows of observation matrix are obtained as follow:

$$[\Psi_{k*i+1}{}^T, \cdots \Psi_{k*i+k}{}^T]^T = \frac{\partial g_{i+1}(\mathbf{F}(\boldsymbol{\rho}, \triangle\mathbf{q}^{i\to i+1}))}{\partial \boldsymbol{\rho}}\Big|_{\rho=\rho_0} \tag{7}$$

These new rows can increase the rank of observation matrix only if they are linearly independent of the other existent rows Ψ_j for $j=1, \cdots, k*i$. The observation matrix including the new rows is

$$\mathbf{J}_{i+1} = [\Psi_1{}^T, \cdots, \Psi_{k*i}{}^T, \Psi_{k*i+1}{}^T, \cdots, \Psi_{k*i+k}{}^T]^T \tag{8}$$

The QR decomposition of $\mathbf{J}_{i+1}{}^T$ is given as:

$$\mathbf{J}_{i+1}{}^T = \mathbf{QR} \tag{9}$$

where $\mathbf{Q}$ is a $(p \times k*(i+1))$ orthogonal matrix and $\mathbf{R}$ is a $(k*(i+1) \times k*(i+1))$ upper triangular matrix. If the columns $\Psi_{k*i+1}{}^T, \cdots, \Psi_{k*i+k}{}^T$ are linearly independent of the left columns, the corresponding diagonal elements of the matrix $\mathbf{R}$ are nonzero. The larger the element is, the more independent the column is. In other words, a larger value offers the more different information to the calibration porcess. The linear independence measure for the configuration χ^{i+1}, which is a function of the free vector $\mathbf{F}$, is defined by summing the reciprocals of corresponding diagonal elements of $\mathbf{R}$:

$$M(\mathbf{F}) = \sum_{j=k*i+1}^{k*i+k} \left(\frac{1}{r_{jj}}\right) \tag{10}$$

Hence, the optimal configuration χ^{i+1} is determined to minimize $M(F)$. If it is divergent, we exclude zero diagonal elements from r_{jj} for $j = k*i+1, \cdots, k*i+k$ and minimize $M(\mathbf{F})$ again. Excluding the zero elements and minimizing $M(\mathbf{F})$ continues until it is convergent. Then Rank $(J_{i+1}) = i*k + (k-t)$ where t is the number of the excluded elements. All the kinematic parameters are identifiable if the rank is equal to the number of parameters.

4. Parameter Observability of the PMC

The PMC (see Fig. 1(a)) is made up of a fixed base, a mobile platform and six linear actuators, LN_i for $i=1, 2, \cdots, 6$. The base connections are composed of Spherical joints (S-joins), while the platform connections are comprised of Universal joints (U-joints). The centers of the S-joints and U-joints are respectively denoted by B_i and P_i for $i=1, 2, \cdots, 6$. The configuration of the PMC is given by a (6×1) vector $\mathbf{q}$ representing the lengths of the linear actuators:

$$\mathbf{q} = [q_1, \cdots, q_6]^T \tag{11}$$

Typically each variable is given as:

$$q_i = q_{off,i} + \triangle q_i \tag{12}$$

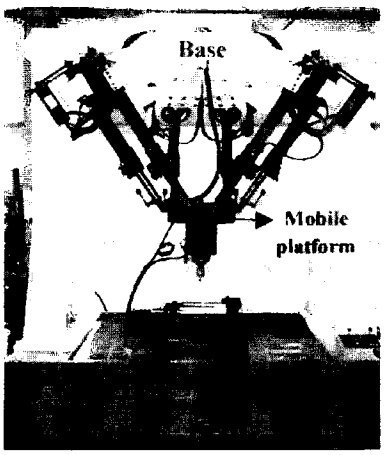

Fig. 1(a) The PMC constructed for a machine tool

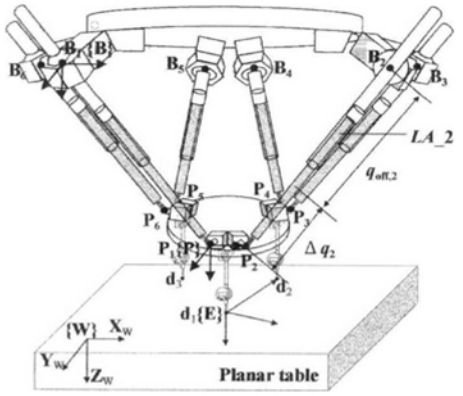

Fig. 1(b) Kinematic structure of the PMC and a single planar table

where $\triangle q_i$ is the linear actuation sensor reading and $q_{off,i}$ is a fixed offset value. We define a Cartesian coordinate frame $\{\mathbf{W}\}$ fixed at the planar table, a frame $\{\mathbf{B}\}$ at the base and a frame $\{\mathbf{P}\}$ at the platform, respectively, as shown in Fig. 1(b):

1) the axes $\mathbf{X}_W$ and $\mathbf{Y}_W$ of frame $\{\mathbf{W}\}$ on the planar table are conveniently chosen by a user and the axis $\mathbf{Z}_W$ is perpendicular to the table.

2) the point B_1 is the origin of frame $\{\mathbf{B}\}$, while the orientation of frame $\{\mathbf{B}\}$ is identical to that of frame $\{\mathbf{W}\}$

3) the point P_1 is the origin of frame $\{\mathbf{P}\}$ and the axis $\mathbf{X}_P$ is determined by $\overrightarrow{P_1P_2}$ and $\mathbf{X}_P\mathbf{Y}_P$ plane is defines as the points P_1, P_2 and P_6 while $\mathbf{Z}_P$ is perpendicular to the table.

From the definitions of $\{\mathbf{B}\}$ and $\{\mathbf{P}\}$ we have:

$$^{B}P_{B1_x}=^{B}P_{B1_y}=^{B}P_{B1_z}=0 \tag{13a}$$

$$\begin{aligned}^{P}P_{P1_x}=^{P}P_{P1_y}=^{P}P_{P1_z}=^{P}P_{P2_y}\\ =^{P}P_{P2_z}=^{P}P_{P6_z}=0\end{aligned} \tag{13b}$$

where $^{i}P_j$ denotes the coordinates of a point j with respect to a frame $\{\mathbf{i}\}$. Supposing that U-joints and S-joints are perfect, we can describe the pose of $\{\mathbf{P}\}$ with respect to $\{\mathbf{W}\}$ by 36 kinematic parameters:

$$\begin{aligned}\boldsymbol{\rho}=[&q_{off,1},\ \cdots,\ q_{off,6},\ ^{B}P_{B2_x},\ ^{B}P_{B2_y},\ \cdots,\ ^{B}P_{B6_z},\\ &^{P}P_{P2_x},\ ^{P}P_{P3_x},\ \cdots,\ ^{P}P_{P6_x},\ ^{P}P_{P6_y},\\ &^{W}P_{B1_x},\ ^{W}P_{B1_y},\ ^{W}P_{B1_z}]\end{aligned} \tag{14}$$

We first examine the parameter observability under three constraint coordinates. As shown in Fig. 1(b), three digital indicators are mounted on a platform to check its movement in $\mathbf{Z}_W$. It isn't necessary that the planar table be parallel to the base because all the kinematic parameters are calibrated with respect to the planar table. At an initial configuration, the frame $\{\mathbf{E}\}$ is defined by the points d_i for $i=1, 2, 3$ representing the center of the contact balls: d_1 is the origin of frame $\{\mathbf{E}\}$, while the $\mathbf{X}_E$ axis is determined by $\overrightarrow{d_1d_2}$ and $\mathbf{X}_E\mathbf{Y}_E$ plane is defined by the points d_1, d_2 and d_3. A (4×4) homogeneous transformation matrix of $\{\mathbf{E}\}$ with respect to $\{\mathbf{W}\}$ is written as

$$^{W}\mathrm{T}_E=^{W}\mathrm{T}_B\ ^{B}\mathrm{T}_P\ ^{P}\mathrm{T}_E=\begin{bmatrix}^{W}\mathbf{R}_E & ^{W}\mathbf{P}_E\\ 0\ 0\ 0 & 1\end{bmatrix} \tag{15}$$

where $^{W}\mathbf{R}_E$ is expressed by a set of Euler angles, i.e., $^{W}\boldsymbol{\Omega}_E=[^{W}\Omega_{E_x},\ ^{W}\Omega_{E_y},\ ^{W}\Omega_{E_z}]^T$. Since the planar table is flat, there is no change in the indicator reading when the frame $\{\mathbf{E}\}$ translates along $\mathbf{X}_W$ and $\mathbf{Y}_W$, and rotates about $\mathbf{Z}_W$. On the contrary, the indicator reading changes when the frame $\{\mathbf{E}\}$ rotates about $\mathbf{X}_W$ and $\mathbf{Y}_W$, and translates along $\mathbf{Z}_W$. Therefore, if the frame $\{\mathbf{E}\}$ moves to any configuration from the initial configuration without changing the readings of all three indicators, the three coordinates $(^{W}\Omega_{E_x},\ ^{W}\Omega_{E_y},\ ^{W}P_{E_z})$ are unchanged while the movement is accomplished by $\mathbf{F}=(^{W}P_{E_x},\ ^{W}P_{E_y},\ ^{W}\Omega_{E_z})$: it can be defined as a *constraint operator*, $\boldsymbol{C}_3=\mathrm{diag}(1, 1, 0, 0, 0, 1)$. The constraint movement of $\{\mathbf{E}\}$ is identical to that of $\{\mathbf{P}\}$, since $^{P}T_E$ is held to fix the pose of $\{\mathbf{E}\}$ referring to $\{\mathbf{P}\}$ as long as the initial configuration is not changed. Eq. (15) is rewritten as

$$^{W}\mathrm{T}_P=^{W}\mathrm{T}_E\ ^{P}\mathrm{T}_E^{-1} \tag{16}$$

where $^{P}T_E$ is defined by setting the digital indicators. This can move the level of constraint plane for a global calibration as shown in Fig. 2: the mobile platform is placed over the entire workspace where the calibration data are taken. Eq. (16) implies that $^{W}\Omega_{P_x}$, $^{W}\Omega_{P_y}$ and $^{W}P_{P_z}$ can be the constraint coordinates instead of $(^{W}\Omega_{E_x},\ ^{W}\Omega_{E_y},\ ^{W}P_{E_z})$ in which case the position vectors of

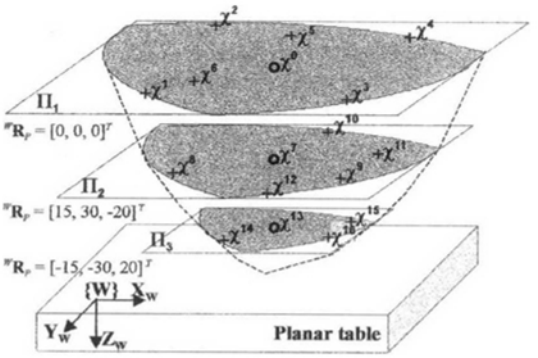

Fig. 2 Three constraint planes defined by changing the height of digital indicators and optimal configurations with same ${}^{W}R_P$ and ${}^{W}P_{P_z}$ on a X-Y plane

digital indicators need not be included. The constraint movement between the configurations $\boldsymbol{\chi}^a$ and $\boldsymbol{\chi}^b$ is given as:

$$C_3[\boldsymbol{\chi}^b(\triangle\mathbf{q}^b, \boldsymbol{\rho}) - \boldsymbol{\chi}^a(\triangle\mathbf{q}^a, \boldsymbol{\rho})] = \begin{bmatrix} {}^{W}\Omega_{P_x}{}^{b} \\ {}^{W}\Omega_{P_y}{}^{b} \\ {}^{W}P_{P_z}{}^{b} \end{bmatrix} - \begin{bmatrix} {}^{W}\Omega_{P_x}{}^{a} \\ {}^{W}\Omega_{P_y}{}^{a} \\ {}^{W}P_{P_z}{}^{a} \end{bmatrix} = \tilde{\mathbf{N}} \tag{17}$$

where ${}^{W}\Omega_{P_x}$, ${}^{W}\Omega_{P_y}$ and ${}^{W}P_{z}$ are computed by the forward kinematics and $\tilde{\mathbf{N}}=[n_1, n_2, n_6]^T=[0, 0, 0]$ under the assumption that the planar table is perfectly flat without measurement noise. The calibration equation is derived by

$$g(\triangle\mathbf{q}^{a-b}, \tilde{\mathbf{N}}, \boldsymbol{\rho}) = \boldsymbol{C}[f(\triangle\mathbf{q}^b, \boldsymbol{\rho}) - f(\triangle\mathbf{q}^a, \boldsymbol{\rho})] - \tilde{\mathbf{N}} = 0 \tag{18}$$

and linearized at $\boldsymbol{\rho}=\boldsymbol{\rho}_0$, which gives the error model as follows:

$$\triangle\mathbf{h} = g(\boldsymbol{\rho}) - g(\boldsymbol{\rho}_0) = \boldsymbol{\Psi}(\boldsymbol{\rho}_0)\triangle\boldsymbol{\rho} \tag{19}$$

where $\boldsymbol{\Psi}(\boldsymbol{\rho}_0)=\nabla g(\boldsymbol{\rho}_0)$, which is the (3×36) sub-matrix of the observation matrix.

To display the optimal configurations on a **X-Y** plane, we find two optimal coordinates ${}^{W}P_{P_x}$ and ${}^{W}P_{P_y}$ out of the free vector $\mathbf{F}=[{}^{W}\Omega_{P_z}, {}^{W}P_{P_x}, {}^{W}P_{P_y}]^T$. If an initial configuration $\boldsymbol{\chi}^0$ is placed on the plane $\prod_1$, the succeeding optimal configurations $\boldsymbol{\chi}^i$ for $i=1, 2, \cdots, 6$ are found. The element $r_{18,18}$ of **R** matrix is zero, when the observation matrix obtained from $\boldsymbol{\chi}^0$ to $\boldsymbol{\chi}^6$ is decomposed to the **QR** matrices. Excluding the zero element $r_{18,18}$ and redefining the independence measure $M(\mathbf{F})$ leads to Rank$(\mathbf{J})=17$ on plane $\prod_1$. As long as the initial configuration $\boldsymbol{\chi}^0$ is held, adding the other configurations can't increase the rank. For the global calibration, configurations $\boldsymbol{\chi}^7$ and $\boldsymbol{\chi}^{13}$ are placed on the planes $\prod_2$ and $\prod_3$, respectively, with the different orientations as shown in Fig. 2. The optimization procedure continues on the planes $\prod_2$ and $\prod_3$ as does the plane $\prod_1$ and finds five and three optimal configurations, respectively. The optimal configurations are evenly distributed over three constraint planes to offer a global calibration. Consequently, the maximum rank is 33. If a coordinate is free to increase the space of **F**, Rank$(\mathbf{J})=27$: it is obtained from only one initial configuration. We get the same Rank$(\mathbf{J})=33$ by adding another initial configuration. All the optimal configurations bring the total rank of the observation matrix to 33 so that three kinematic parameters can't be identified under the *constraint operator* $\boldsymbol{C}_3$.

The QR-decomposition of observation matrix indicates that diagonal elements from 34-th to 36-th of **R** matrix are zero. This implies that ${}^{W}P_{B1_x}$, ${}^{W}P_{B1_y}$ and ${}^{W}P_{B1_z}$ are non-identifiable parameters, which have no effects on the constraint movements. It is noted that calibrating the non-identifiable parameters isn't necessary because the orientation of $\{\mathbf{B}\}$ is identical to that of $\{\mathbf{W}\}$: the PMC can meet the straightness, flatness and perpendicularity defined by the frame $\{\mathbf{W}\}$ even though it machines a workpiece with respect to $\{\mathbf{B}\}$. Hence, ${}^{W}P_{B1_x}$ ${}^{W}P_{B1_y}$ and ${}^{W}P_{B1_z}$ are assigned as arbitrary coordinates.

The movements under $\boldsymbol{C}_3$ is somewhat complicated. To make them simple, we adopt the *constraint operator* $\boldsymbol{C}_1=\text{diag}(0, 0, 0, 0, 0, 1)$: only one coordinate ${}^{W}P_{P_z}$ is constrained and checked by an indicator. The origin of frame $\{\mathbf{E}\}$ is fixed at a contact ball while the orientation of $\{\mathbf{E}\}$ is identical to that of frame $\{\mathbf{P}\}$. Since the position of the indicator is associated with the constraint movements, the augmented kinematic parameters, i.e., $\boldsymbol{\rho}_a=[{}^{P}P_{E_x}, {}^{P}P_{E_y}, {}^{P}P_{E_z}]^T$, must be added to bring the number of kinematic parameters to 39.

We can find 35 optimal configurations from

only one initial configuration because the d.o.f. of the free vector is increased : $\mathbf{F}=[{}^{W}\Omega_{E_x}, {}^{W}\Omega_{E_y}, {}^{W}\Omega_{E_z}, {}^{W}P_{E_x}, {}^{W}P_{E_y}]^T$. Adding initial configurations no longer increases the number of optimal configurations.

The QR-decomposition indicates that ${}^{B}P_{B2_y}$, ${}^{W}P_{B1_x}$, ${}^{W}P_{B1_y}$ and ${}^{W}P_{B1_z}$ can't be identified. The parameters ${}^{W}P_{B1_x}$, ${}^{W}P_{B1_y}$ and ${}^{W}P_{B1_z}$ are determined as the same way as C_3 and the parameter ${}^{B}P_{B2_y}$ is decided by the redefined frame $\{\mathbf{B}\}$: point b_2 is defined as the projected point of B_2 to the plane $\mathbf{X}_B\mathbf{Y}_B$ which is parallel to the $\mathbf{X}_W\mathbf{Y}_W$ and the axis $\mathbf{X}_B$ is determined by $\overrightarrow{B_1b_2}$. This definition yields

$$ {}^{B}P_{B2_y}=0 \tag{20}$$

This reduces the number of kinematic parameters to 35. The orientation of $\{\mathbf{B}\}$ isn't equal to that of $\{\mathbf{W}\}$ while the axis $\mathbf{Z}_B$ is identical to the axis $\mathbf{Z}_W$. Therefore, the PMC can't meet the straightness defined by $\{\mathbf{W}\}$ but the perpendicularity and the flatness can be accomplished when the PMC machines the workpiece with respect to $\{\mathbf{B}\}$.

5. Calibration of PMC

Before the calibration, the repeatability and the accuracy of the PMC are examined. We substitute the designed parameters into a kinematic model and measure the positioning and straightness errors. The platform moves 300 mm in the $\overrightarrow{X_W}$, $\overrightarrow{Y_W}$ and $\overrightarrow{X_WY_W}$ directions and return to initial position. These movements are repeated three times and the position and the straightness of a target mounted on the platform are measured by a laser sensor. As shown in Fig. 3, all the positioning errors increase over 2500 μm but decrease back to zero. If a platform approaches the position in the same direction, the repeatability is 10 μm, but it is 100 μm in a different direction. The offset of 100 μm comes from the backlashes at the joints.

The calibration method is applied to the PMC. A planar table has a flatness of 5 μm over 500$\times$ 500 mm^2 and the digital indicators (Weihua and Mills, 1999) have 1 μm-resolution and 25 mm-stroke. The platform moves to successive configurations under position control. When the changes of all the indicator's readings are within ± 2 μm, $\triangle\mathbf{q}$ is acquired for the calibration data. Since the number of calibration equations must be more than four times the number of parameters, we add the augmented configurations to the constraint planes of Fig. 2 and take 60 configurations for C_3 and 180 configurations for C_1. The constraint movements under C_3 are generated by changing the direction of the mobile

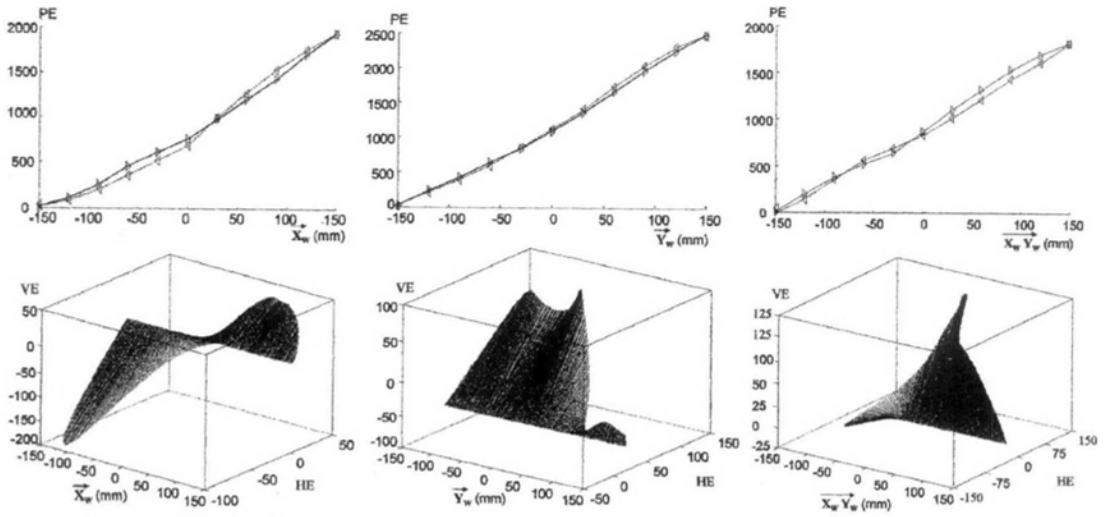

PE : Positioning error (μm), HE : Horizontal straightness error (μm), VE : Vertical straightness error (μm)

Fig. 3 Positioning and straightness errors in the $\overrightarrow{X_W}$, $\overrightarrow{Y_W}$ and $\overrightarrow{X_WY_W}$ directions

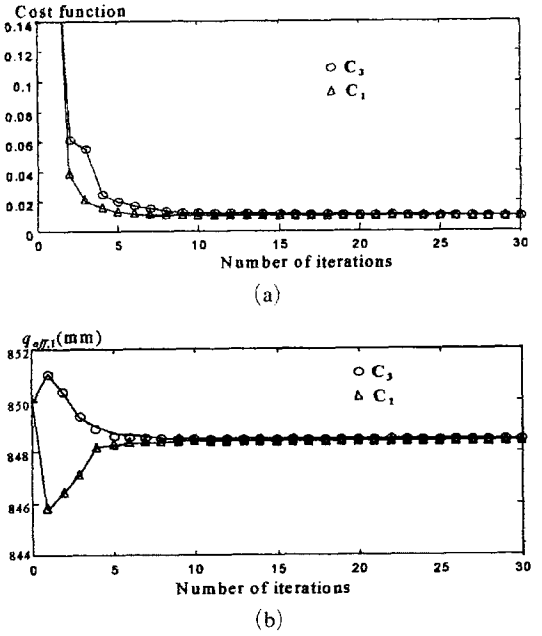

Fig. 4 (a) Cost function versus number of iterations (b) Convergence of $q_{off,1}$ under C_1 and C_3

platform two or three times, while the movements under C_1 can be generated at once. Figs. 4(a) and 4(b) depict the convergent trends of cost function and parameter $q_{off,1}$ for each *constraint operators*. Although the operators C_3 and C_1 produce different sets of calibration data, we can get the identical sets of kinematic parameters. This verifies that the calibration method is reliable.

There is 2-3 mm difference between the calibrated parameters and the designed ones. The calibration reduces the positioning error to 130 μm. Furthermore, all the errors are within 150 μm overall the workspace, which indicates that the proposed method accomplishes the global calibration. However, there is no improvement in the straightness errors, which are owing to non geometric parameters such as noise, backlash and etc. rather than the calibration method. These results shows that a parallel mechanism can easily be calibrated by a planar table and digital indicators. However, we still have many problems to be solved before applying the PMC to the MC. They will be the elaborate manufacturing/assembling of parts, accurate manufacturing of fixtures, cancelling of measurement noises, compensating of backlashes, etc..

6. Conclusion

This paper examines the parameter observability of the PMC using optimal calibration configurations. The QR-decomposition is used to find the optimal calibration configurations which maximize the linear independence of rows of an observation matrix. The linear independence measure is defined by summing the reciprocals of diagonal entries of the **R** matrix. We applied two *constraint operators*, which constrain the mobile platform to three or five coordinates by a planar table and digital indicators. All the necessary kinematic parameters assigned in the PMC are identifiable and convergent to desirable accuracy. This eliminates the concern over the poor parameter observability due to the constrained movements and the local calibration due to a single planar table. Although the constraint operators offer different sets of calibration data, we can get the identical sets of kinematic parameters. However, the errors are too large to apply the PMC for the MC. This is owing to the non geometric parameters rather than the calibration method. It is concluded that the proposed calibration method is an effective, low cost and feasible technique for a Parallel typed Machining Center in an industrial environment.

Acknowledgment

This work was supported (in part) by the Korea Science and Engineering Foundation (KOSEF) through the Machine Tool Research Center at Changwon National University.

References

Besnard, S. and Khalil, W., 2001, "Identifiable Parameters for Parallel Robots Kinematic Calibration," *in Proc. IEEE Int. Conf. Robot. Automat.*, Seoul, Korea, pp. 2859~2866.

Borm, J. H. and Menq, C. H., 1991, "Determination of Optimal Measurement Configurations

for Robot Calibration Based on Observability Measure," *Int. J. Robot. Res.*, Vol. 10, No. 1, pp. 51~63.

Desnard, S. and Khalil, W., 1999, "Calibration of Parallel Robots Using two Inclinometers," *Proc. of the 1999 IEEE Int. Conf. on Robot. Automat.* Detroit, Michigan, pp. 1758~1763.

Hunt, K. H., 1978, *Kinematic geometry of mechanisms*, Oxford Univ. Press.

Menq, C. H. Borm, J. H. and Lai, J. Z., 1989, "Identification and Observability Measure of a Basis set of Error Parameters in Robot Calibration," duddl*A*SME J. Mech. Trans. Automat. Design, Vol. III, No. 4, pp. 513~518.

Masory, O. and Jiahua, Y., 1995, "Measurement of Pose Repeatability of Stewart Platform," *J. Robot. Syst.* Vol. 12, No. 12, pp. 821~832.

Weihua, X. and Mills, J. K., 1999, "A New Approach to the Position and Orientation Calibration of Robots," *in Proc. IEEE Int. Symposium on Assembly and Task Planning Porto*, Portugal, Jul., pp. 268~273.

Zhuang, H., Li, B., Roth, Z. S. and Xire, X., 1992, "Self-calibration and Mirror Center Offset Elimination of a Multi-beam Laser Tracking System," *Robot. Autonomous Syst.*, Vol. 9, pp. 255~269.

Zhuang, H. Masory, O. and Yan, J., 1995, "Kinematic Calibration of Stewart Platform Using Pose Measurements Obtained by a Single Theodolite," *Proc. IROS*, pp. 329~335.